Laboratori Nazionali di Frascati

LNF-67/71

E. P. Balsamo, C. Guaraldo and R. Scrimaglio : A SECONDARY EMISSION MONITOR FOR ELECTRON BEAMS OF HIGH ENERGY AND INTENSITY.

Estratto da : Nuclear Instr. and Meth. 55, 339 (1967)

NUCLEAR INSTRUMENTS AND METHODS 55 (1967) 339–343; © NORTH-HOLLAND PUBLISHING CO.

A SECONDARY EMISSION MONITOR FOR ELECTRON BEAMS OF HIGH ENERGY AND INTENSITY

E. P. BALSAMO, C. GUARALDO and R. SCRIMAGLIO
Laboratori Nazionali del CNEN, Frascati, Roma, Italy

Received 11 May 1967

A secondary emission device is described. It is able to detect position and profile of an electron beam of high intensity and energy in its transport magnetic channel.

Prototype characteristics with associated electronic circuits for signal pick-up and experimental results obtained with the 400 MeV electron and positron linac of the Laboratori Nazionali di Frascati del CNEN (LNF) are also reported.

Experimental results at a primary's energy of 400 MeV are compared with a theoretical calculation based on the Møller cross-section for the electron-electron scattering, keeping into account, at the thicknesses involved in the device, other contributions like those from electromagnetic showers and tertiary electrons.

1. Introduction

The utilization of a device that allows direct monitoring of position and profile of an electron beam of high intensity and energy in several points of a magnetic channel is subjected to various requirements:

1. Proportionality between intensity of output signal and beam intensity;

2. Good sensitivity, meant as minimum current density detectable with the tv camera that monitors the "optical-cell";

3. Small mean square angle of multiple scattering of the particles traversing the detector;

4. Resistance against radiation damage, etc.

ZnS targets and plastics, quartz and gas scintillators do not satisfy all these requirements [1]). In particular ZnS targets have an extremely short life at the current levels normally involved in linacs: normally the life expected with a current of a few $\mu A/cm^2$ is of some hours (the LNF linac mean electron current density is about 30 $\mu A/cm^2$); this fact imposes the use of an automatic target exchanger.

A way which seems to be satisfactory is one involving the use of Čerenkov gas cells (He or Ar at atmospheric pressure), equipped with two thin Al windows and a mirror, made of thin Al, which reflects the Čerenkov light [1, 2]).

The sensitivity is high: the argon Čerenkov cells used at Stanford with the Mark IV have allowed to detect current levels as low as 0.1 $\mu A/cm^2$, corresponding to about 1/500 of the maximum current, using a vidicon tv camera placed 3 m apart from the cell. There is rigorous proportionality between signal intensity and beam intensity (this can give, for instance, a measure of the spread of the electron density over the beam section), a small multiple scattering angle (for energies higher than some GeV) and long duration.

On the other hand, the high intensity of the beam imposes a very refined shielding of the tv circuit. The camera will result very resistant to radiations when a quartz window vidicon is used; the approximate estimation of radioactivity developed by a collimator which absorbs the whole electromagnetic shower gives [3]) values of about 10^9 erg/g in 10 year at a distance of 3 m: a quartz window vidicon will work still efficiently after having absorbed 10^{11} erg/g of radiation. The electronic circuit components seem to be resistant to γ-ray radiation of 10^{10} erg/g. However, the lens system remains the weak point of the camera and data on its resistance to radiations are not reliably known.

For the Ar cells, in the "hot areas" Corning glass 7940 (i.e. high purity quartz) must be used for the windows; Corning glass is very expensive and thermal effects which can hurt either the window or the reflecting glass should not be disregarded.

Moreover, with a 400 MeV beam, like that of LNF linac, an Ar cell 25 cm long with a total Al thickness of 9.1 mg/cm^2 gives a multiple scattering angle of 2.51×10^{-2} rad: 10 times greater than the maximum allowable angular spread of the beam in the cell.

Using an H_2O cell with water circulating to eliminate heating phenomena, gives an additional increase of the scattering angle.

In conclusion, the problems concerned with the use

of a visual detector for monitoring position and profile of a highly intensive and energetic electron beam, have advised us to develop a secondary emission device, the efficiency and detecting characteristics of which will be described.

The device (fig. 1) is made of two wires at right angle and moving simultaneously through the beam: the current intensity of secondary electrons emitted is proportional to the part of the wire that collides with the beam, and once the beam has been centered with respect to the wires, it is possible to obtain directly from the current signal the beam profile in a median cross section [4]).

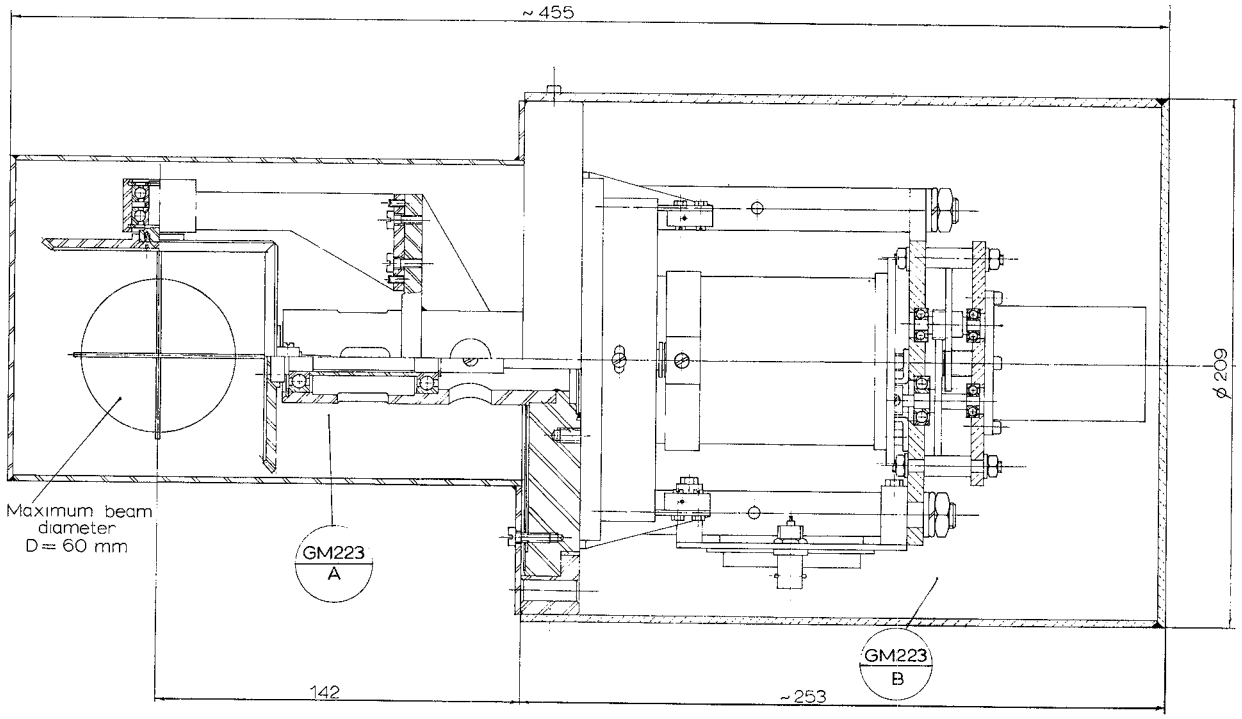

Fig. 1. Mechanical drawing of the monitor.

2. Calculation of secondary emission at high energies

The efficiency for the production of secondary electrons has been calculated taking into account the following contributions:

1. Secondary electrons emitted directly from the matter with an output probability which depends from their point and energy of creation;

2. Tertiary electrons produced from the secondary ones in the wire, which diffuse towards the surface and undergo an exponential absorption law;

3. Compton electrons from γ-rays lost from the electromagnetic shower originated from the incident primary electrons.

2.1. Directly emitted secondary electrons

The cylindrical wire of our device has been approximated by a thin indefinite plane lamina of width ξ equal to the diameter of the wire. In the calculation of the probabilities that a secondary electron has to leave the wire, considering the creation point, it is possible to compensate the error introduced by this approximation [5]).

Having weighted the contributions from the various parts of the lamina and in the hypothesis that the secondary electrons loose energy according to Whiddington's law [6]):

$$W^2 - W^2(s) = as, \tag{1}$$

where s is the abscissa and for a one has:

$$a/\rho = 0.4 \times 10^{12}\ (\mathrm{eV})^2\ \mathrm{g}^{-1}\ \mathrm{cm}^2, \quad (\text{with } \rho = \text{density}),$$

the number of secondaries per incident primary, i.e. the efficiency, is:

$$Y_s = \rho(N/A)Z\left\{2\int_{I_{ion}}^{\beta}\int_0^R [d\phi(T, W)/dW] \times [\tfrac{1}{2}(R-x)/R]dW\,dx + 2\int_{\beta/\sqrt{2}}^{\beta}\int_0^{\xi-R} [d\phi(T, W)/dW] \times [\tfrac{1}{2}(R-x)/R]dW\,dx + \int_{\beta/\sqrt{2}}^{\beta}\int_{\xi-R}^{R} (d\phi/dW)[(R-\tfrac{1}{2}\xi)/R]dW\,dx + \int_{\beta/\sqrt{2}}^{\frac{1}{2}T}\int_0^{\xi} (d\phi/dW)[(R-\tfrac{1}{2}\xi)/R]dW\,dx\right\}, \quad (2)$$

where $\beta = (a\xi)^{\frac{1}{2}}$ and ρ, Z, A are respectively the density, atomic number and atomic weight of the matter used for the wire; N is Avogadro's number; $d\phi(T, W)$ is the Møller cross section for the emission of secondary electrons caused by a non-polarized electron passing through the matter; R is the range of the secondary and x its point of creation.

In the computation of Y_s we will consider the energy of primaries in the range 60–1500 MeV and thicknesses from 5×10^{-2} cm to 1.5×10^{-1} cm; neglecting terms of the order of 10^{-4} and smaller, we obtain for the efficiency in the directly emitted secondary electrons:

$$Y_s = (2mc)^2\{\pi r_c^2(N/A)Z\}\rho\{(2a)^{-1}[3\{(a\xi)^{\frac{1}{2}}-I_{ion}\} + 2T\ln|\{T-(a\xi)^{\frac{1}{2}}\}/\{T-I_{ion}\}|]+\tfrac{5}{6}(\xi/a)^{\frac{1}{2}}\}. \quad (3)$$

2.2. Contribution of tertiary electrons

The contribution of tertiary electrons has been estimated in accordance with the theory of Baroody [7]), formulated on the basis of Sommerfeld's free electron model, which, at the low energies involved in the process, keeps qualitatively into account the most meaningful experimental results.

Keeping again into account the probability a tertiary has to leave the matter in the considered geometry and in the hypothesis of an exponential absorption, we obtain for the efficiency:

$$Y_t = \alpha\{\ln|\tfrac{1}{2}T/I_{ion}|+\ln|\tfrac{1}{2}T/(T-I_{ion})| + \{2-T/(T-I_{ion})\}+[(\tfrac{1}{2}T)^2-(I_{ion})^2/(2T^2)]\}, \quad (4)$$

where

$$\alpha = 2mc^2\{\pi r_c^2(N/A)Z\}\{2BE_f^{\frac{3}{2}}/(\phi a)\}(2/\sigma)\rho, \quad (5)$$

where B is a constant approximately equal to 2.95×10^8 $(eV)^{\frac{1}{2}}$/cm; E_f is the Fermi energy, ϕ the work function and σ is 10^{-6}/cm.

2.3. Production of Compton electrons

As regards the estimate of electrons that can be originated by the Compton effect from a piece of matter when traversed by a primary electron beam of high energy, the electromagnetic shower generated must be considered.

Using the Crawford and Messel tables relative to electrons in the energy range of 50–1000 MeV in Pb [8]) for the energy lost to the shower as γ radiation, and with some approximations [see ref.[5])], we can estimate the production of Compton electrons.

Keeping again in mind that for an electron leaving the wire, the point of production must be taken into account, we obtain for the efficiency:

$$Y_c = \rho(N/A)ZY_\gamma\sqrt{2} \times \int_0^{T_s}\int_0^R \{d\sigma(T, \varepsilon_\gamma)/dT\}\{\tfrac{1}{2}(R-x)/R\}dx\,dT, \quad (6)$$

where $d\sigma(T, \varepsilon_\gamma)$ is the Compton cross-section as a function of the emitted electron energy T:

$$d\sigma(T, \varepsilon_\gamma)/dT = \{\pi r_c^2mc^2/(\varepsilon_\gamma-T)^2\}\{[mc^2T/\varepsilon_\gamma^2]^2 + 2[(\varepsilon_\gamma-T)/\varepsilon_\gamma]^2+[(\varepsilon_\gamma-T)/\varepsilon_\gamma^3][(T-mc^2)-m^2c^4]\}, \quad (7)$$

Y_γ is the efficiency for the production of γ's by the incident primary.

2.4. Numerical results

We give in table 1 the calculated partial efficiencies Y_s, Y_t, Y_c and the total efficiency Y for some values of the primaries energies in the range 60–1000 MeV and for thicknesses of 1.5×10^{-1} and 1×10^{-1} cm of W.

Table 1

E_p (MeV)	ξ (cm)	Y_s	Y_t	Y_c	Y
60	1.5×10^{-1}	2.18×10^{-1}	4.67×10^{-3}	1.04×10^{-1}	3.26×10^{-1}
	1.0×10^{-1}	1.78×10^{-1}	4.67×10^{-3}	1.04×10^{-1}	2.87×10^{-1}
200	1.5×10^{-1}	2.19×10^{-1}	5.18×10^{-3}	1.28×10^{-1}	3.52×10^{-1}
	1.0×10^{-1}	1.79×10^{-1}	5.18×10^{-3}	1.28×10^{-1}	3.12×10^{-1}
400	1.5×10^{-1}	2.19×10^{-1}	5.47×10^{-3}	1.31×10^{-1}	3.55×10^{-1}
	1.0×10^{-1}	1.79×10^{-1}	5.47×10^{-3}	1.31×10^{-1}	3.15×10^{-1}
1000	1.5×10^{-1}	2.19×10^{-1}	5.86×10^{-3}	1.33×10^{-1}	3.58×10^{-1}
	1.0×10^{-1}	1.79×10^{-1}	5.86×10^{-3}	1.33×10^{-1}	3.18×10^{-1}

3. Secondary emission device prototype description

The monitor prototype has been made of stainless steel with "Capton" windows, while for the pick-up W, wires of 1 mm dia. have been used.

The motion of the wires is provided by a gears

decoupled dc motor, controlled by a solid-state servo amplifier.

The servo amplifier is triggered, for the reversing of the motor motion, by pulses obtained from two photo-transistors excited by the light of a filament lamp mounted on a cam that rotates with the wires.

The sweep speed of the wires can easily be changed by varying the voltage supplied to the stator of the motor. The necessity of varying the wires speed arises from the fact that the pulse repetition frequency of the electron beam may vary between large values and that to obtain a correctly interpretable image of the beam a sufficient number of coordinates must be measured. The output signal is represented by a sequency of fast pulses and to obtain a good image on the CRO screen we can use either an electronic integrator or direct pulse display.

The electronic integrator gives a dc output proportional to the peak value of the pulses or, in other words, it lengthens the pulse duration so as to make them well visible on the screen; this method may give wrong informations when the pulse height is decreasing at a rate greater than the discharge time constant of the integrator.

In the second case (the direct display) the CRO beam intensity is strongly increased while displaying the pulses and reduced when the base-line is being displayed; this leads to an image of the ordinates being measured.

This last method should be preferred to the first one when sudden variations in the profile of the pulse amplitude are expected.

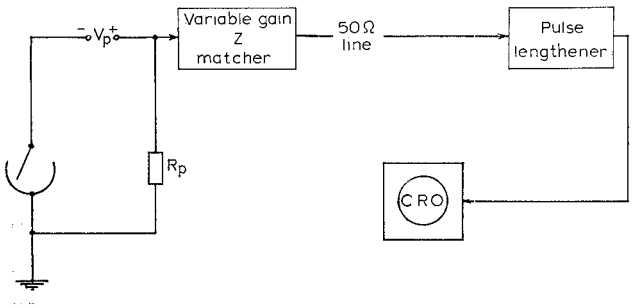

Fig. 2. Pick-up circuit for the signal.

The pick-up circuit for the signal is shown in fig. 2. A negative voltage of about 200 V is applied to the wires; the current signal due to the secondary emission appears as a positive voltage across the resistor R_p. A variable gain impedance matcher connects the signal source to 50 ohm coaxial cable used to feed the oscilloscope.

3.1. Beam positioning

One of the purposes of the monitor is to center the beam with respect to the collimator holes. To perform correctly this operation some mean should be given to the operator, to know exactly the actual position of the centers of the collimators. This mean is represented in our device by a gate-signal generated in a way similar to that used to drive the servo amplifier by a lamp mounted on the wires cam. The electron beam will be centered when the beam signal will coincide with the reference gate. The actual gate width is 18 mm.

3.2. Sensitivity of the monitor

The factors limiting the sensitivity of the monitor are the thermal noise (Johnson effect) of pick-up resistor and noise due to line power and power circuits for acceleration of the beam.

A frequency band limitation may considerably reduce all these kinds of noise; supposing to use a pick-up resistor R_p of 10^4 ohm and a frequency band limited to 1.6 MHz, for allowing a good reproduction of the shortest pulses normally used in linacs ($\tau \geqq 1\ \mu s$), the thermal noise will result in some tens of μV.

In order to reduce strongly the induced noise, a lower limit could be introduced in the frequency band, so to keep out of it the line frequency, with its 2nd and 3rd harmonics and the frequency corresponding to the pulse repetition rate of the accelerated beam; this last frequency generally does not exceed 500 cps. A refined shielding of the device should not be neglected to keep noise at a minimum.

Considering the induced noise of the same order of magnitude of thermal noise we can fix a threshold of 100 μV with a satisfactory signal-to-noise ratio.

The corresponding minimum detectable beam current is

$$(i_p)_{min} \simeq 0.6 \mu A.$$

4. Experimental results

In fig. 3 is the LNF linac beam photograph taken at the input of our monitor, after having passed 0.16 g/cm^2 of aluminum, on which an electroluminescent film has been laid and 15 cm of air. The beam energy is 456 MeV and the peak current is 10 mA with a 25 cps repetition rate. Since the beam has a high intensity,

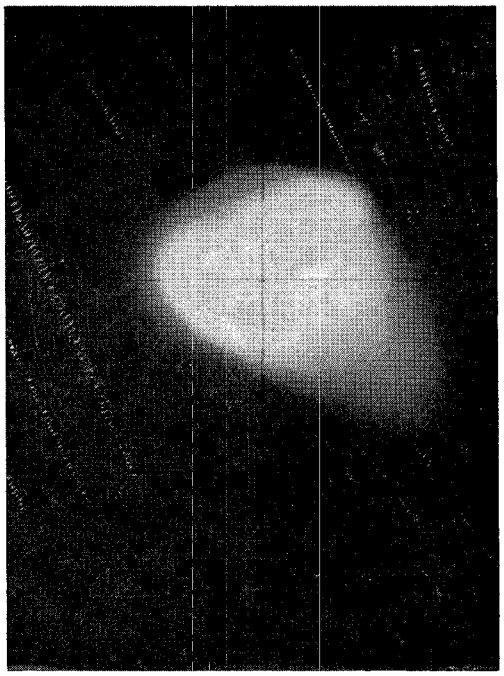

Fig. 3. Beam photo of the LNF linac.

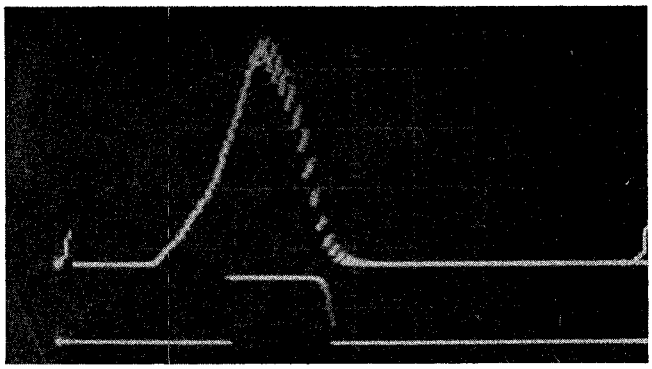

Fig. 4. Oscillogram of the signal corresponding to the x direction sweep.

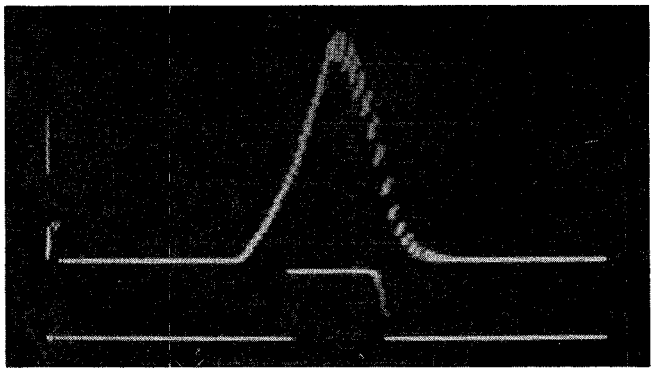

Fig. 5. Oscillogram of the signal corresponding to the y direction sweep.

the picture, taken by exposing to a beam pulse a common photographic emulsion, does not reproduce unequivocally the effective shape of the beam cross section.

In fig. 4 is the oscillogram of the monitor signal corresponding to the sweep in the x direction; the resulting width of the beam is $\simeq$ 3 cm and the peak value of the beam is about 3 mm out of center, as results also in fig. 3.

The oscillogram of the signal corresponding to the sweep in the y direction is reported in fig. 5. The beam width is of 2.8 and its symmetry with respect to the x axis is confirmed by the coincidence of the peak value with the collimator (gate) center.

In conclusion it can be said that also on the basis of an approximate shape of the beam as that which appears in fig. 3, our monitor characterizes with good precision its longitudinal and cross dimensions, is able to individualize a shifting with respect to the axis of the transport line and allows to go back to the beam shape by an analysis of the signal.

The experimental efficiency has been computed, utilising the data of fig. 5 and integrating the secondary current represented by the profile of the signal reported; the resulting charge Q_s has then been divided by the peak primary beams charge so obtaining the experimental efficiency $Y_{exp} \simeq 35\,\%$; this value is in good accordance with our theoretical calculations which are $Y_{th} \simeq 32\,\%$ (table 1).

It is a pleasure to thank Mr. S. Faini for the design of the whole mechanics of the device, Mr. A. Botticelli for prototype studies and Prof. C. Castagnoli, G. Sacerdoti and C. Schaerf for useful discussions.

References

[1]) B. de Raad, TN-64-4 (1964).
[2]) B. de Raad, TN-64-12 (1964).
[3]) H. De Staebler, TN-63-69 (1963).
[4]) G. Hortig, Nucl. Instr. and Meth. **30** (1964) 355.
[5]) E. P. Balsamo, C. Guaraldo and R. Scrimaglio, Report LNF-66/66 (1966).
[6]) V. J. Vanhuyse and R. E. Van de Vijver, Nucl. Instr. and Meth. **15** (1962) 63.
[7]) E. M. Baroody, Phys. Rev. **78** (1950) 780.
[8]) D. F. Crawford and H. Messel, Phys. Rev. **128** (1962) 2352.